Journal of Magnetic Resonance 195 (2008) 153–161

Contents lists available at ScienceDirect

Journal of Magnetic Resonance

journal homepage: www.elsevier.com/locate/jmr

The effect of experimental parameters on the signal decay in double-PGSE experiments: Negative diffractions and enhancement of structural information

Noam Shemesh, Yoram Cohen *

School of Chemistry, The Raymond and Beverly Sackler Faculty of Exact Sciences, Tel Aviv University, Ramat Aviv, Tel Aviv 69978, Israel

ARTICLE INFO

Article history:
Received 24 July 2008
Revised 31 August 2008
Available online 17 September 2008

Keywords:
Double-pulsed gradient spin echo
Double PGSE
d-PGSE
Diffusion
Confined geometries
Nerve phantom
Restriction
Micro-compartments

ABSTRACT

Double pulsed gradient spin echo (d-PGSE) experiment has been recently suggested for detecting microscopic anisotropy in macroscopically isotropic samples. This sequence is complex and has many variables, including, intra alia, combinations of directions and amplitudes of the pulsed gradients, diffusion times in each of the encoding periods and the mixing time period. The effect of these experimental parameters of the d-PGSE sequence was studied in an array of water filled microcapillaries of micron diameters. We found that negative diffractions occur, as indeed predicted by recently published simulations. We also found differential effects of prolongation of the mixing time between collinear and orthogonal d-PGSE experiments. The d-PGSE experiment in the collinear direction perpendicular to the long axis of the cylinder exhibited a marked dependence on the mixing time, while the orthogonal d-PGSE experiment exhibited no such dependence at all. Interestingly, one of the most important predictions by the simulations was that the d-PGSE sequence could potentially discriminate between compartments of different sizes better than the single PGSE (s-PGSE) and it seems that our experimental results indeed corroborate these predictions.

1. Introduction

Measurement of translational motion by MR techniques has provided the ability to non-invasively explore microscopic characteristics of opaque samples. The main advantage of diffusion MR is that it measures the mean displacement of a species at a given diffusion time in a completely non-perturbing way by directionally tagging the nucleus of interest [1,2]. In isotropic non-restricted systems, the mean displacement is proportional to the diffusion coefficient which, in turn, is proportional to the effective size of the diffusing moiety and can therefore be used to investigate a multitude of samples ranging from simple molecules to complexes, supramolecular systems and complex mixtures of compounds [3–5]. When the molecules are confined to certain geometries, they undergo restricted diffusion. Therefore, when the molecule is observed after a sufficiently long diffusion time to probe the boundaries of the restricting compartment, only an apparent diffusion coefficient (ADC) can be obtained from the root mean square displacement (rmsd). Since MR techniques measure the rmsd of molecules, it is clear that under certain conditions one may be able to infer from such data the compartment size and shape, which are usually smaller than the voxel size in MR measurements. Indeed, diffusion MR was used in recent years to elucidate structure in porous materials [6], polymers [7], and biological tissues, including white matter (WM) in neuronal tissue [8].

Pulsed gradient spin echo (PGSE) experiments [1,2] have been used extensively to study molecular displacement in confined geometries and micro-compartments [6]. One of the most intriguing observations arising from PGSE experiments is the diffusive-diffraction phenomenon obtained when the signal decay of spins undergoing restricted diffusion is plotted against $\mathbf{q}$ ($\mathbf{q} = \frac{1}{2\pi} \cdot \gamma\delta\mathbf{G}$) [9–14].

It was found that the size of the compartment may be extracted from either the diffraction dip or the probability distribution function (PDF) obtained after $E(\mathbf{q})$ is Fourier transformed (FT) with respect to $\mathbf{q}$ [15]. This is due to the fact that under certain experimental conditions the diffusion-driven attenuation curve $E(\mathbf{q})$ holds a Fourier relation with the average propagator $\overline{P}(R, \Delta)$ [15]. Exact solutions for $E(\mathbf{q})$ have been obtained, over the years, for important geometries such as arrays of rectangular walls [16], cylinders, and spheres [11,14,17]. The simulations for these geometries have been corroborated experimentally [18], and even corrected for diverging from the short gradient pulse (SGP) approximation [13,14,17–19]. The effect of various parameters has been studied systematically [20,21] and provided insight to the nature of attenuation profiles. Avram et al. showed that the rotational angle has a dramatic effect on the loss of diffraction patterns [21]. This study also showed that the structural information obtained from the diffusion–diffraction dips and from the PDF

* Corresponding author. Fax: +972 3 6407469.
E-mail address: ycohen@post.tau.ac.il (Y. Cohen).

1090-7807/$ - see front matter © 2008 Elsevier Inc. All rights reserved.
doi:10.1016/j.jmr.2008.09.006

obtained by the Fourier transform (FT) of the signal decay, were the same [21]. This is important since q-space diffusion MR, which had been used to study red blood cells [22,23] has recently been used to study neuronal tissue and WM in the central nervous system, both in vitro and in vivo [24–32]. In these cases, diffractions were not observed, probably due to the distribution of axon sizes [18,27,33]. Most of the applications of diffusion MR and MRI in material science, biological science and medical science have used a single PGSE (s-PGSE) experiment. The double PGSE (d-PGSE) sequence (Fig. 1) was first proposed in [34] and studied theoretically by Mitra [35]. The d-PGSE sequence was initially used mostly pertaining to flow phenomena [36,37], velocity correlation [38] and suppression of convection artifacts [39]. This sequence has been shown to enable the detection of local diffusion anisotropy in macroscopically isotropic systems [40] and has recently gained attention regarding its ability to probe such effects in biological systems [41,42]. The d-PGSE sequence employs two diffusion sensitizing pairs of gradients, which may be applied either collinearly or with any angle between them, and are separated by a mixing time (t_m). It was shown that comparison of collinear and orthogonal d-PGSE experiments makes it possible to probe microscopic anisotropy in macroscopically isotropic samples [40–42]. This has recently been used to probe anisotropy in gray matter (GM) and in a GM phantom [41,42].

Very recently, simulations of the attenuation profile of multiple-PGSE experiments in confined geometries have been presented by Özarslan and Basser [43,44], showing theoretically that some of the limitations of s-PGSE may be overcome by using the d-PGSE experiments, most notably the ability to obtain diffractions in samples comprised of compartments of different sizes, due to the zero crossings of the signal [43]. This may be of importance, since biological tissues are characterized by variable sizes.

To the best of our knowledge, a comprehensive study of the effect of the various parameters of the d-PGSE sequence on the attenuation profile in ordered micro-scale systems has not been preformed yet. The d-PGSE is a versatile sequence with many parameters that may affect the diffusion–diffraction pattern in such diffusion experiments. The effect of some of these parameters on the signal decay in multiple PGSE experiments was theoretically analyzed by Özarslan and Basser, with intriguing results regarding the diffusion–diffraction phenomenon [43].

In this study, we sought to reveal the effect of the variation of the parameters on the signal decay in d-PGSE sequence that had been performed on a controlled system of water-filled microcapillaries. In view of the potential of the d-PGSE experiment to detect local anisotropy in macroscopically isotropic systems [41,42], we evaluated the effects of the most relevant parameters, i.e., the mixing time, the different diffusion times and the different pulsed gradients directions (orthogonal and collinear) in the high q regime. Finally, we studied samples of mixtures of microcapillaries with different sizes, and compared the results with those of the s-PGSE experiments.

2. Materials and methods

All measurements were preformed on a Bruker 8.4 T NMR spectrometer capable of producing up to 190 G/cm in each direction. The sequence was written in-house and calibrated.

Hollow microcapillaries with diameters of 15, 20 or 29 μm (Polymicro Technologies, USA) or mixtures thereof were immersed in water for a period of several days, prior to each experiment. The microcapillaries were packed into a 4 mm glass sleeve which was inserted into a 5 mm NMR tube, aligned with the main axis parallel to the z-direction of the magnet. For mixture samples, microcapillaries were counted to comprise the correct volumetric ratio. Typical linewidths of 5–10 Hz were obtained after shimming.

The d-PGSE experiment is depicted in Fig. 1. The terminology used in this paper will be s-PGSE$_i$ where i indicates the direction of the diffusion encoding for a single PGSE experiment, and d-PGSE$_{mn}$, where m and n indicate the pulse gradients directions of the first and second diffusion period, respectively, for the double-PGSE sequence. For instance, a d-PGSE$_{xz}$ experiment will indicate a d-PGSE experiment comprised of diffusion sensitizing gradients in orthogonal sense where the first pair of diffusion encoding gradients $\mathbf{G}_1$ is in the x-direction with gradient duration δ_1 and diffusion period Δ_1, and the second pair of diffusion encoding gradient $\mathbf{G}_2$ is in the z-direction with gradient duration δ_2 and diffusion period Δ_2. In all of the experiments in this study, the amplitudes of the diffusion sensitizing gradients were chosen to be identical i.e., $|\mathbf{G}_1| = |\mathbf{G}_2|$. The mixing time ($t_m$) is defined as the interval between the end of the first diffusion encoding period and the beginning of the second diffusion encoding period. It is important to note that using the sequence shown in Fig. 1, the mixing time cannot effectively be set to 0 and must at least have the length of δ_1 which in this study was 2 ms. In combination with echo timing and eddy current considerations, the minimum mixing time in the present study was set to 5 ms, and TE_1 and TE_2 were always chosen to be unequal, to avoid overlapping echoes.

The data from the experiments were magnitude-calculated to correct for the negative diffractions that had been obtained (vide infra). The data were Fourier transformed using OriginLab software. Diameters were extracted from either the diffraction dips ($\mathbf{q}_{min}$) from the graph of E_q/E_0 versus $\mathbf{q}_{eff}$ or from the full-width at half-maximum (FWHM), obtained from the FT of E_q/E_0 versus $\mathbf{q}_{eff}$. The sizes were taken as $1.22/\mathbf{q}_{min}$ or 1.22^*FWHM, respectively [14,21] to correct for the cylinder geometry of our microcapillaries.

Since we wanted to directly compare the d-PGSE and s-PGSE methods, and because the first minimum of the d-PGSE signal occurs at the half of the q of the s-PGSE minimum (vide infra), we defined an effective $\mathbf{q}$ for the d-PGSE experiment, $\mathbf{q}_{eff}$, such that the diffractions from the two experiments occur at the same q_{eff}:

$$|\mathbf{q}_{eff}| = \left|\frac{1}{2\pi}\gamma\delta\mathbf{G}_1\right| + \left|\frac{1}{2\pi}\gamma\delta\mathbf{G}_2\right| \quad (1)$$

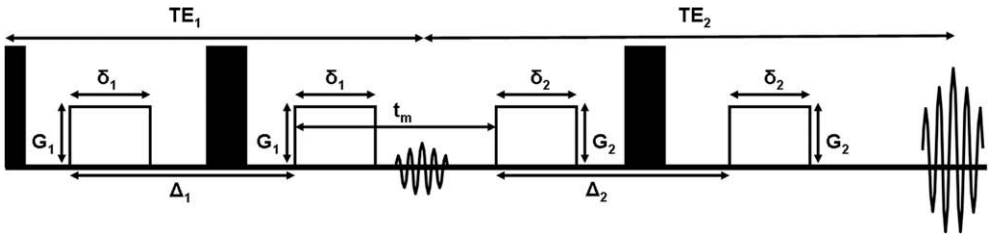

Fig. 1. The d-PGSE sequence. Two pairs of directionally independent diffusion sensitizing gradients $\mathbf{G}_1$ and $\mathbf{G}_2$ are applied for lengths of δ_1 and δ_2, respectively, with diffusion times of Δ_1 and Δ_2 and are separated by a variable mixing time (t_m).

2.1. Calibration experiment

A ~1:1 volumetric *tert*-butyl alcohol:D_2O (Sigma–Aldrich) mixture in a 5 mm NMR tube was used for the calibration experiments. The measurements were conducted on the non-exchanging methyl protons. d-PGSE experiments were conducted in 10 collinear, orthogonal, and polar combinations of directions. Thirteen q_{eff} values were collected with G_{max} = 81 G/cm, $\delta_1 = \delta_2$ = 2 ms, resulting in a maximal q_{eff} of 1379 cm^{-1}, $\Delta_1 = \Delta_2$ = 100 ms and t_m of 100 ms. The number of scans (NS) was 8.

For the comparison of s-PGSE and d-PGSE, 29 μm microcapillaries were used. The parameters for the d-PGSE$_{xx}$ experiment were as follows: 32 points were collected with G_{max} = 100 G/cm, $\delta_1 = \delta_2$ = 2 ms, resulting in a maximal q of 851 cm^{-1}, $\Delta_1 = \Delta_2$ = 150 ms and t_m of 5 ms. The number of scans (NS) was 128. For the s-PGSE$_x$ experiment, 32 points were collected with G_{max} = 100 G/cm, δ = 4 ms, resulting in a maximal q of 1703 cm^{-1}, Δ = 150 ms. The number of scans (NS) was 32.

2.2. Negative diffraction experiments

In these experiments, ensembles of 29 μm microcapillaries were used. The parameters of the d-PGSE$_{xx}$ experiment were as follows: a total of 32 q values were collected with, G_{max} = 100 G/cm, $\delta_1 = \delta_2$ = 2 ms, resulting in a maximal q_{eff} of 1703 cm^{-1}, $\Delta_1 = \Delta_2$ = 150 ms, and t_m of 5 or 50 ms, and with NS of 128. The reference s-PGSE$_x$ scan consisted of 32 q values with G_{max} = 100 G/cm, δ = 4 ms, resulting in a maximal q of 1703 cm^{-1} and with Δ = 150 ms (sufficiently long to probe the boundaries). The number of scans was 64.

2.3. The effect of prolonging the mixing time

Experiments were performed on 29 μm microcapillaries. For the collinear d-PGSE$_{xx}$ experiments, 32 q values were collected with G_{max} = 100 G/cm, $\delta_1 = \delta_2$ = 2 ms, resulting in a maximal q_{eff} of 1703 cm^{-1}, $\Delta_1 = \Delta_2$ = 150 ms, with NS of 128. The mixing time was varied between 5 and 150 ms. For the orthogonal d-PGSE$_{xz}$, the same parameters were used, however, in these experiments, Δ_2 was set to 10 ms.

2.4. The effect of prolonging the diffusion periods

This set of experiments was performed on 20 μm microcapillaries. For both the collinear d-PGSE$_{xx}$ and the orthogonal d-PGSE$_{xz}$ experiments, 24 q values were collected with G_{max} = 120 G/cm, $\delta_1 = \delta_2$ = 2 ms, resulting in a maximal q_{eff} of 2043 cm^{-1}, and t_m of 5 ms and the diffusion periods were varied. The NS was 256. The reference s-PGSE$_x$ experiment was conducted with the following parameters: 32 q values were collected with G_{max} = 120 G/cm with δ = 4 ms, resulting in maximal q of 2043 cm^{-1}, Δ = 100 ms, with NS of 128. In some s-PGSE experiments, 32 q values were collected with G_{max} = 180 G/cm and δ = 4 ms, resulting in a maximal q of 3065 cm^{-1}, Δ = 100 ms, and NS in these experiments was 128.

The same parameters were used to test the effect of the order of the gradients used in the orthogonal d-PGSE$_{xz}$ and d-PGSE$_{zx}$ experiments on 20 μm microcapillaries.

2.5. Discrimination between sizes in mixtures of two sizes of microcapillaries

2.5.1. 20:29 μm 1:1 volumetric mixture

The d-PGSE$_{xx}$ experiments were conducted with the following parameters: 32 q values were collected with G_{max} = 100 G/cm $\delta_1 = \delta_2$ = 2 ms, resulting in a maximal q_{eff} of 1703 cm^{-1}, Δ_2 was set to 150 ms and Δ_1 was varied. The mixing time was set to 5 ms with NS of 128. The parameters of the s-PGSE$_x$ experiment were as follows: 32 q values were collected with G_{max} = 100 G/cm and with δ of 4 ms, resulting in a maximal q of 1703 cm^{-1}, Δ was set to 150 ms, and NS was set to 32.

2.5.2. 15:20 μm 3:1 volumetric mixture

The d-PGSE$_{xx}$ experiments were conducted with the following parameters: 32 q values were collected with G_{max} = 120 G/cm, $\delta_1 = \delta_2$ = 2 ms, resulting in a maximal q_{eff} of 2043 cm^{-1}, Δ_2 was set to 100 ms and Δ_1 was varied. For each Δ_1 the mixing time was set to 5, 25 or 100 ms, and NS was set to 160. The parameters of the s-PGSE$_x$ were as follows: 32 q values were collected with G_{max} = 120 G/cm and with δ = 4 ms, resulting in a maximal q of 2043 cm^{-1}, and Δ was set to 110 ms, and NS was set to 64.

For all of the experiments, the signal-to-noise (SNR) ratio of the first point (q = 0 cm^{-1}) was on the order of several thousands. In all of these experiments, the echo times were chosen to be the shortest possible.

3. Results and discussion

3.1. Calibration experiment

First, we sought to determine that our hardware and software were performing satisfactorily in the d-PGSE experiments. For this purpose, diffusion of *tert*-butyl alcohol in a 5 mm NMR tube was measured. Since this sample is isotropic, we expected the same attenuation curves when different combinations of diffusion directions were applied. We tested 10 collinear, orthogonal and polar combinations of gradients. Fig. 2A shows the normalized signal attenuation (E_q/E_0) versus q_{eff}^2 obtained from these experiments. Indeed, our sequence provided the same results for any combination of directions, as expected from an isotropic sample.

Fig. 2B shows the signal decay as function of q^*a for the d-PGSE$_{xx}$ and the s-PGSE$_x$ experiment. As expected [43], the first minimum of the d-PGSE$_{xx}$ occurs at q^*a = 0.61, while the first minimum of the s-PGSE occurs at q^*a = 1.22, which is also where the second diffraction of the d-PGSE$_{xx}$ occurs.

3.2. Negative diffraction experiments

Özarslan and Basser [43] predicted that the attenuation profile from d-PGSE$_{xx}$ experiment should yield negative diffractions when performed in restricted compartments. Fig. 3 shows the attenuation of the signal from water in the d-PGSE$_{xx}$ experiment, with diffusion periods sufficiently long to probe the boundaries of the 29 μm microcapillaries ($\Delta_1 = \Delta_2$ = 150 ms). When the mixing time is minimal (5 ms), sharp negative diffractions are observed (Fig. 3A). The first diffraction is negative and very strong, whereas the second (positive) and third (negative) diffractions are much weaker. We note that the first negative diffraction can be readily seen even with NS = 1 (data not shown). When the mixing time is prolonged, the sharpness of the diffractions is somewhat reduced (Fig. 3B). The s-PGSE$_x$ experiment (Fig. 3C) reveals the standard positive diffractions observed from these microcapillaries. Such sharp negative diffractions were also obtained from 15 and 20 μm microcapillaries (data not shown).

Fig. 3 shows that the negative diffraction is stronger and more sharp than the diffraction in the s-PGSE experiment. The sharpness of the negative diffractions probably occur because of the zero crossing [43]. In s-PGSE, the signal at the q_{min} is significantly attenuated, however, in d-PGSE experiments, the zero crossing forces the signal to be zero. Therefore the diffraction is sharper.

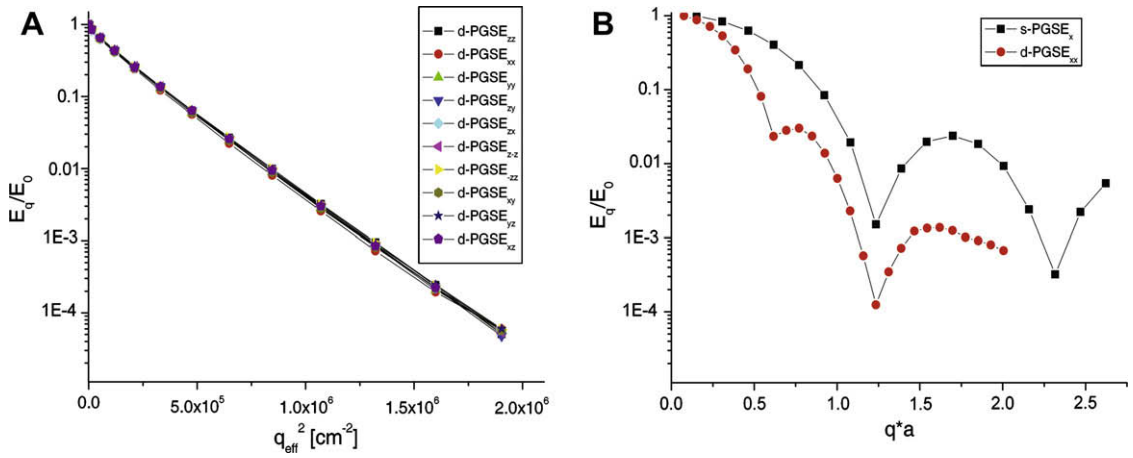

Fig. 2. (A) Calibration of the d-PGSE sequence. Normalized signal decay (E_q/E_0) versus q_{eff}^2 values of a sample of *tert*-butyl alcohol in 10 collinear, orthogonal and polar directions in the d-PGSE experiment. The same linear attenuation which was obtained from all directional pairs indicates that the gradients are well calibrated and that the sequence is performing properly. (B) Comparison of the signal decay in s-PGSE$_x$ (black) and d-PGSE$_{xx}$ (red) experiments performed on 29 μm microcapillaries. The signal decay is plotted versus q^*a. The first diffraction minimum of the d-PGSE$_{xx}$ experiment occurs at half of that of the s-PGSE$_x$. (For interpretation of color mentioned in this figure the reader is referred to the web version of the article.)

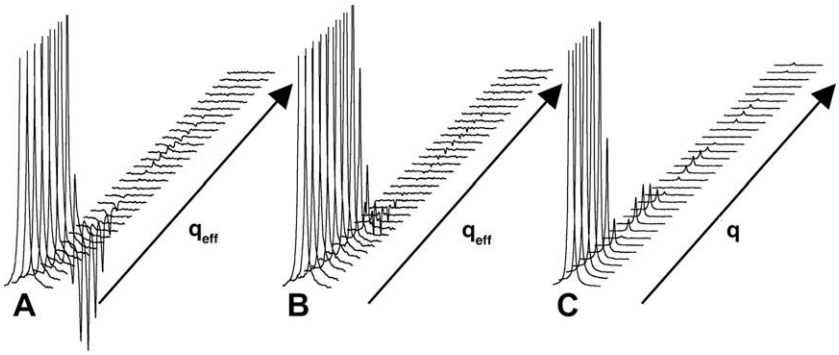

Fig. 3. Negative diffractions observed in d-PGSE$_{xx}$ experiments performed on 29 μm microcapillaries. Signal decay as a function of $\mathbf{q}_{eff}$ when (A) t_m = 5 ms (B) t_m = 50 ms. (C) The reference s-PGSE$_x$ experiment. The vertical display is the same for all figures. Note that the s-PGSE stackplot is plotted versus q.

3.3. The effect of prolonging the mixing time

Fig. 4 shows the signal decay and the displacement profile obtained from the FT of the signal decay obtained for 29 μm microcapillaries in the d-PGSE$_{xx}$ experiment (Fig. 4A and B, $\Delta_1 = \Delta_2 = 150$ ms) and d-PGSE$_{xz}$ (Fig. 4C and D, $\Delta_1 = 150$ ms $\Delta_2 = 10$ ms) experiments with several mixing times. We found that in the d-PGSE$_{xx}$ experiments, the signal attenuation is markedly effected by prolonging the mixing time. The first diffraction dip becomes less pronounced as the mixing time is prolonged. The s-PGSE$_x$ experiment yields the first diffraction dip at $q = 426$ cm^{-1}, and the second diffraction dip at $q = 799$ cm^{-1}, which correspond to a size of 29 and 30 μm, respectively. The d-PGSE$_{xx}$ experiment with the minimal mixing time yields the same first diffraction. The second diffraction is at $q_{eff} = 852$ cm^{-1} which yields a size of 29 μm. However, prolonging the mixing time to 30 ms shifts the first diffraction dip to $q_{eff} = 531$ cm^{-1}, from which a smaller size of 23 μm was extracted, whereas the second diffraction remained nearly unchanged (Fig. 4A). Further prolongation of the mixing time results in a gradual loss of the first (negative) diffraction, but has only a marginal effect on the second (positive) diffraction which remains at the same q values. The effect of the mixing time prolongation in the d-PGSE$_{xx}$ experiment is summarized in Fig. 4E (black squares), which shows the sizes extracted from the FT of the signal decay. Prolonging the mixing times reduces the apparent size of the compartment and eventually an asymptotic value of the compartment size is approached. This resembles the effect anticipated when long diffusion weighting gradient pulses are used in a s-PGSE$_x$ experiment (i.e., long δ) [11,18,21,27]. A smaller apparent size is extracted when the diffusion weighting pulses are effectively long, as non-negligible diffusion occurs during the encoding period [11,18,21,27]. Thus, prolonging the mixing time (t_m in Fig. 1) in the d-PGSE$_{xx}$ sequence appears as an effective addition to δ, although it is probably due to the loss of correlation between the diffusion periods. It is interesting to note that the first diffraction is the one which is sensitive to the prolongation of the mixing time, and that the second diffraction is unaffected throughout the experiment, as indeed was predicted by the Özarslan and Basser [43] paper. This sensitivity is probably due to the zero crossing between the positive and negative signal.

Prolonging the mixing time in the orthogonal d-PGSE$_{xz}$ experiments hardly influences the signal decay or the displacement profile obtained from the FT of the signal decay (Fig. 4C and D). Although Δ_1 had been set to 150 ms, sufficiently long to probe the 29 μm boundaries and Δ_2 had been only 10 ms long, only the second diffraction dip was observed at $q_{eff} = 852$ cm^{-1}. The results of the rmsd obtained from the displacement profile from the d-PGSE$_{xz}$ experiment are summarized in Fig. 4E (red circles). The same effects were also observed from 20 μm microcapillaries (data not shown).

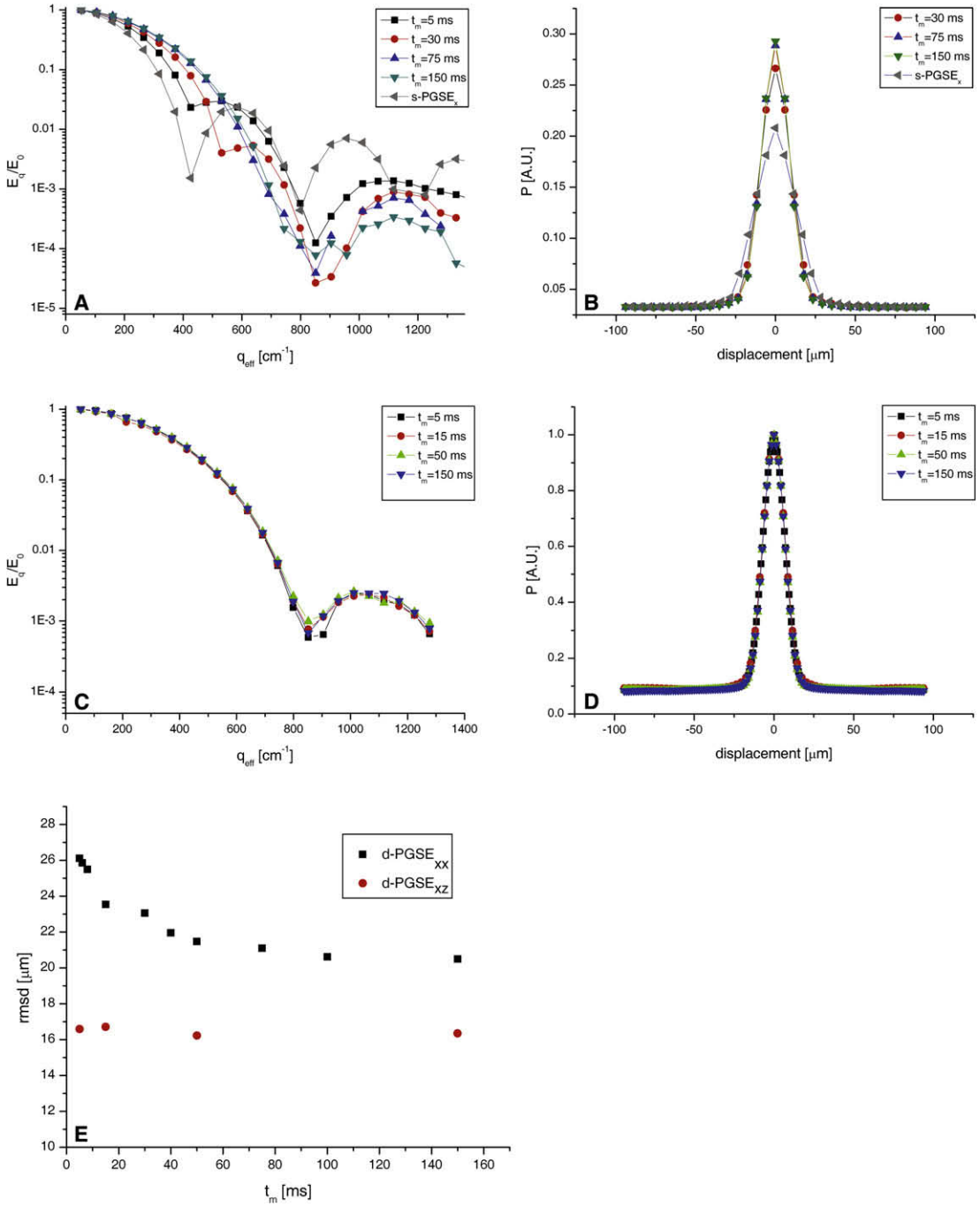

Fig. 4. Signal decay as a function of q_{eff} at different mixing times (A and C) and the FT of the signal decay (B and D) in d-PGSE experiments performed on 29 μm microcapillaries. (A and B) d-PGSE$_{xx}$ experiments with $\Delta_1 = \Delta_2 = 150$ ms with different mixing times. (C and D) d-PGSE$_{xz}$ with $\Delta_1 = 150$ ms and $\Delta_2 = 10$ ms at different mixing times. (E) Summary of the compartment sizes extracted from the d-PGSE$_{xx}$ (black squares) and d-PGSE$_{xz}$ (red circles) experiments obtained from the displacement profile (taken as 1.22°FWHM). Note that the s-PGSE results are plotted versus q. (For interpretation of color mentioned in this figure the reader is referred to the web version of the article.)

From the comparison of d-PGSE$_{xx}$ and d-PGSE$_{zx}$ experiments, it seems that the motional correlation is retained in the collinear directions that are perpendicular to the main axis of the microcapillary, due to the same restriction that the molecules experience in both encoding periods. In orthogonal d-PGSE experiments, restricted motion along the x-direction and free diffusion along the z-direction are indeed not correlated; therefore the correlation is lost, manifested in the very rapid signal decay and in the independence of the extracted size on the t_m.

3.4. The effect of prolonging the diffusion periods

Other important parameters that may affect the results of d-PGSE experiments are the diffusion times Δ_1 and Δ_2. Fig. 5 shows the effect of changing the diffusion periods in d-PGSE experiments performed on 20 μm microcapillaries. Fig. 5A and B reveals that in the d-PGSE$_{xx}$ experiments, prolonging the diffusion periods results in a more efficient probing of the boundaries, until they are probed completely. When $\Delta_1 = \Delta_2 = 10$ ms, a signal decay corresponding

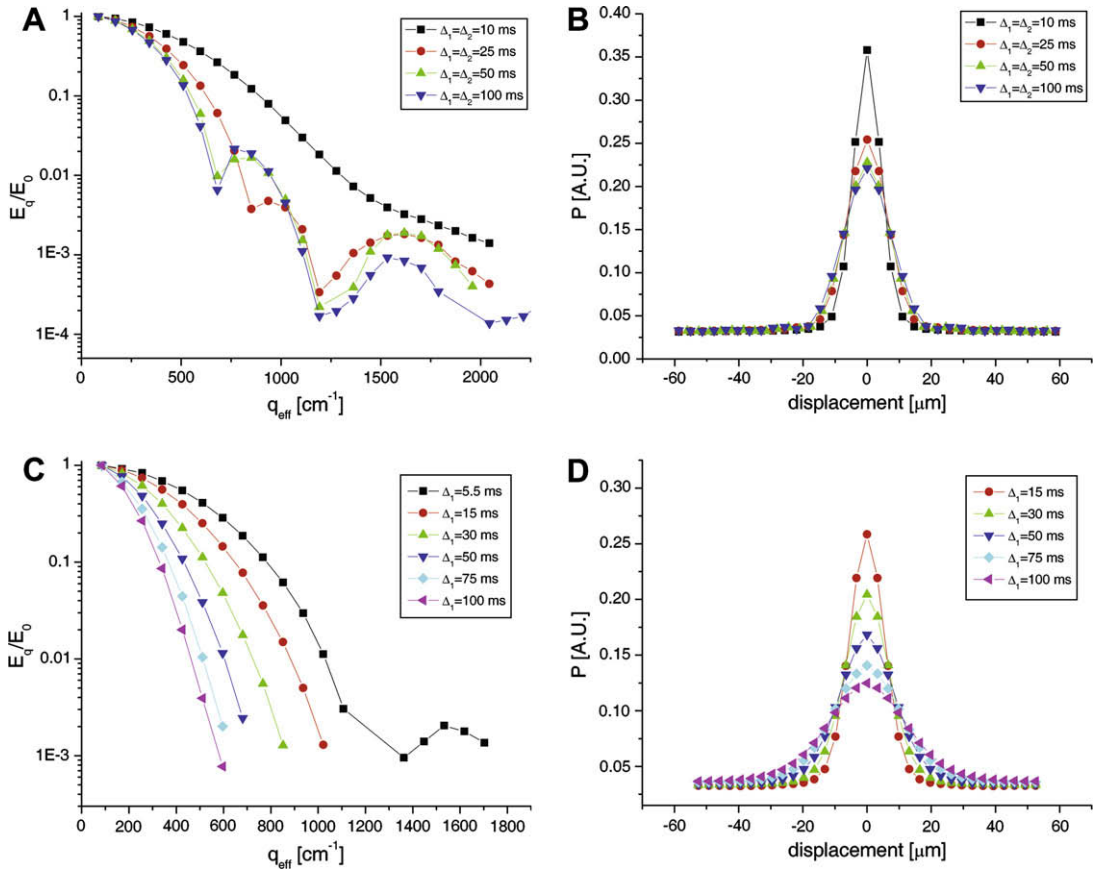

Fig. 5. Signal decay as a function of q_{eff} at different diffusion times (A and C) and the FT of the signal decay (B and D) in d-PGSE experiments performed on 20 μm microcapillaries. (A and B) d-PGSE$_{xx}$ experiments and (C and D) d-PGSE$_{zx}$ experiments with Δ_2 = 100 ms. For all of these experiments, the mixing time was set to 5 ms.

to non-restricted diffusion is observed. When both diffusion periods (i.e., Δ_1 and Δ_2) were prolonged to 25 ms, 50 ms, and then to 100 ms, the same second diffraction dip at q_{eff} = 1192 cm^{-1} which corresponds to 20 μm was observed. However, the first diffraction dips in the d-PGSE$_{xx}$ experiments were observed at q_{eff} = 851 cm^{-1} when the experiments were performed with $\Delta_1 = \Delta_2$ = 25 ms and at q_{eff} = 681 cm^{-1} when the experiments were performed with $\Delta_1 = \Delta_2$ = 50 ms, corresponding to sizes of 14 and 18 μm, respectively. For $\Delta_1 = \Delta_2$ = 50 ms and $\Delta_1 = \Delta_2$ = 100 ms, the same signal decay was observed, and the same structural parameters were extracted, indicating complete probing of the boundaries. The s-PGSE$_x$ reference experiment exhibits diffractions at q = 596 and 1192 cm^{-1} from which a compartment size of 20.5 μm was extracted. The smaller sizes obtained from the d-PGSE$_{xx}$ experiment

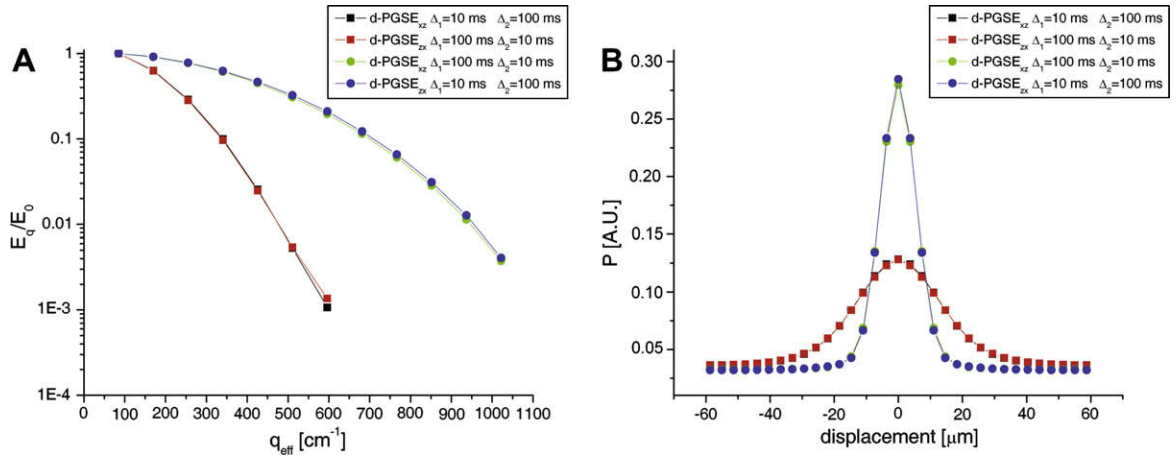

Fig. 6. Signal decay as a function of q_{eff} (A) and the FT of the signal decay (B) in orthogonal d-PGSE experiments performed on 20 μm microcapillaries. The squares represent the experiments with the longer diffusion period in the *z*-direction and the circles represent the experiments with the longer diffusion period in the *x*-direction. (A) d-PGSE$_{xz}$ experiments with Δ_1 = 10 ms and Δ_2 = 100 ms (black squares) and the d-PGSE$_{zx}$ experiment with Δ_1 = 100 ms and Δ_2 = 10 ms (red squares). The complementary d-PGSE$_{xz}$ experiment with Δ_1 = 100 ms and Δ_2 = 10 ms (green circles) and the d-PGSE$_{zx}$ experiment with Δ_1 = 10 ms and Δ_2 = 100 ms (blue circles). In all experiments, the mixing time was set to 5 ms. (For interpretation of color mentioned in this figure the reader is referred to the web version of the article.)

are attributed to the fact that we have used a finite mixing time, which, in fact, acts as an effective addition to δ, thus increasing the violation of the SGP approximation. Interestingly, once the diffractions occur, it seems that the second diffraction remains constant, whereas the first (negative) diffraction is much more sensitive to the boundaries.

Prolonging the diffusion period in the z-direction in the orthogonal d-PGSE$_{zx}$ experiment, i.e., with Δ_2 = 100 ms in the x-direction (sufficiently long to probe the boundaries) with the minimal mixing time, reveals a rapid loss of the diffraction patterns (Fig. 5C and D). When Δ_2 = 5.5 ms, the second diffraction is still observed. However, the first diffraction is completely lost even at this short diffusion period in the z-direction. The FT plots show an increased rmsd with increased Δ_2, indicating a 'free' diffusion behavior. It seems that under these experimental conditions, the contribution of the free diffusion to the attenuation profile apparently supersedes that of the restricted diffusion in this system. Considering the substantial dephasing of spins in a free diffusion mode, this may be expected. The rapid loss of the first diffraction indicates the sensitivity to directional correlation which is probably due to the zero crossings of the signal [43].

3.5. The effect of changing the order of the diffusion sensitizing gradients

We also compared the results from d-PGSE$_{xz}$ and d-PGSE$_{zx}$ experiments, performed with one long diffusion period (sufficiently long to probe the boundaries) and one short diffusion period, with a minimal mixing time of 5 ms. For the d-PGSE$_{xz}$ experiment, where the longer diffusion period comes first and is in the axis perpendicular to the main axis of the cylinder, a restricted profile is expected. For the d-PGSE$_{zx}$ experiment (where the diffusion periods remained the same and the directions of the gradients were swapped) an unrestricted pattern is expected, as the longer diffusion period is now in the direction of the main axis of the cylinder. Fig. 6 shows the results of these experiments. Indeed, for the d-PGSE$_{xz}$ experiments with the long diffusion period in the x-direction i.e., Δ_1 = 100 ms, the attenuation profile and the displacement profile extracted from the FT of the signal decay (green circles) showed characteristics of restricted diffusion, although no diffractions were observed. The size extracted for the 20 μm microcapillaries was 13.7 μm, that is, smaller than the compartment size. When the d-PGSE$_{zx}$ experiment was performed and the long diffusion period was in the z-direction, the contribution of the free diffusion was much larger, as expected (red squares). The size that was extracted from the displacement profile obtained from the FT of the signal decay was 32 μm, indeed, much larger than the diameter of the microcapillaries used in the experiment.

When we performed the complementary experiments, i.e., the d-PGSE$_{zx}$ experiment with the long diffusion period in the x-direction (Δ_2 = 100 ms) (Fig. 6, blue circles), we observed the same signal decay, as in the d-PGSE$_{xz}$ experiment with Δ_1 = 100 ms. Likewise, we observed the same diffusion characteristics of unrestricted diffusion in the d-PGSE$_{xz}$ experiment with Δ_2 = 100 ms (Fig. 6, black squares) as in the d-PGSE$_{zx}$ experiment with Δ_1 = 100 ms, where the long diffusion periods were in the z-direction. These data indicate that the order in which the gradients are applied does not play a role with regard to the signal decay. The same results were obtained with mixing times of 15 and 30 ms (data not shown), indicating once more, that the mixing time has a marginal effect on the signal decay in orthogonal d-PGSE experiments.

3.6. Discrimination between sizes in mixtures of two different sizes of microcapillaries

The s-PGSE$_x$ has only a limited ability to discern between combinations of different sizes embedded within a heterogeneous sample. Very recent simulations suggested that the d-PGSE sequence should have increased sensitivity towards such combinations of sizes. Therefore, we used two mixture samples, a 1:1 29:20 μm (Fig. 7) and a 3:1 15:20 μm (Fig. 8) samples. Both samples were initially studied by the d-PGSE$_{xx}$ sequence with $\Delta_1 = \Delta_2$ = 150 ms, and $\Delta_1 = \Delta_2$ = 100 ms, correspondingly, with the notion that this would be sufficient to probe the boundaries of both sizes in the two samples, and obtain increased sensitivity towards the combination of sizes. However, under these conditions ($\Delta_1 = \Delta_2$ = 150 ms, and $\Delta_1 = \Delta_2$ = 100 ms and t_m = 5 ms), we did not observe any discrimination between the compartments, and although the signal attenuation had not been identical to that of the s-PGSE$_x$ reference scan, we could not discern the two sizes in each sample (Figs. 7A and B and 8A and B). However, in the case of the first mixture, when we set Δ_2 to 150 ms and changed Δ_1 from 6 to 150 ms, while t_m was 5 ms, we first observed a gradual appearance of two diffraction dips, becoming most pronounced at Δ_1 = 50 ms, then a gradual disappearance of the diffraction patterns (Fig. 7A) as Δ_1 was further increased. The most pronounced diffraction dips were observed at q_{eff} = 585 and 1011 cm^{-1}, respectively, corresponding to sizes of 21.0 and 12.0 μm. Interestingly, the ratio of the extracted sizes

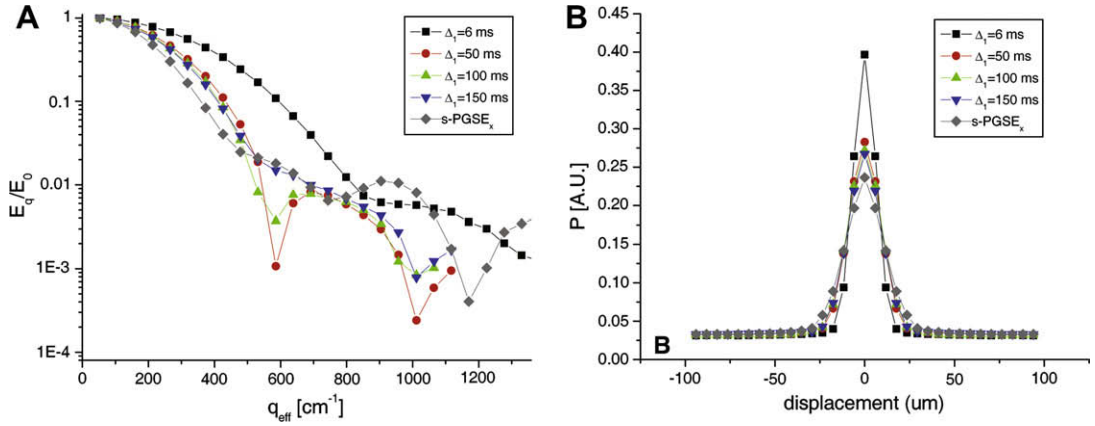

Fig. 7. Signal decay as a function of q_{eff} (A) and the FT of the signal decay (B) of d-PGSE experiments performed on a sample containing a mixture of 1:1 29:20 μm microcapillaries. The first diffusion period was varied while Δ_2 was set to 150 ms, and the mixing time was set to 5 ms. The results from the s-PGSE$_x$ experiment are also shown. Note that the s-PGSE results are plotted versus q.

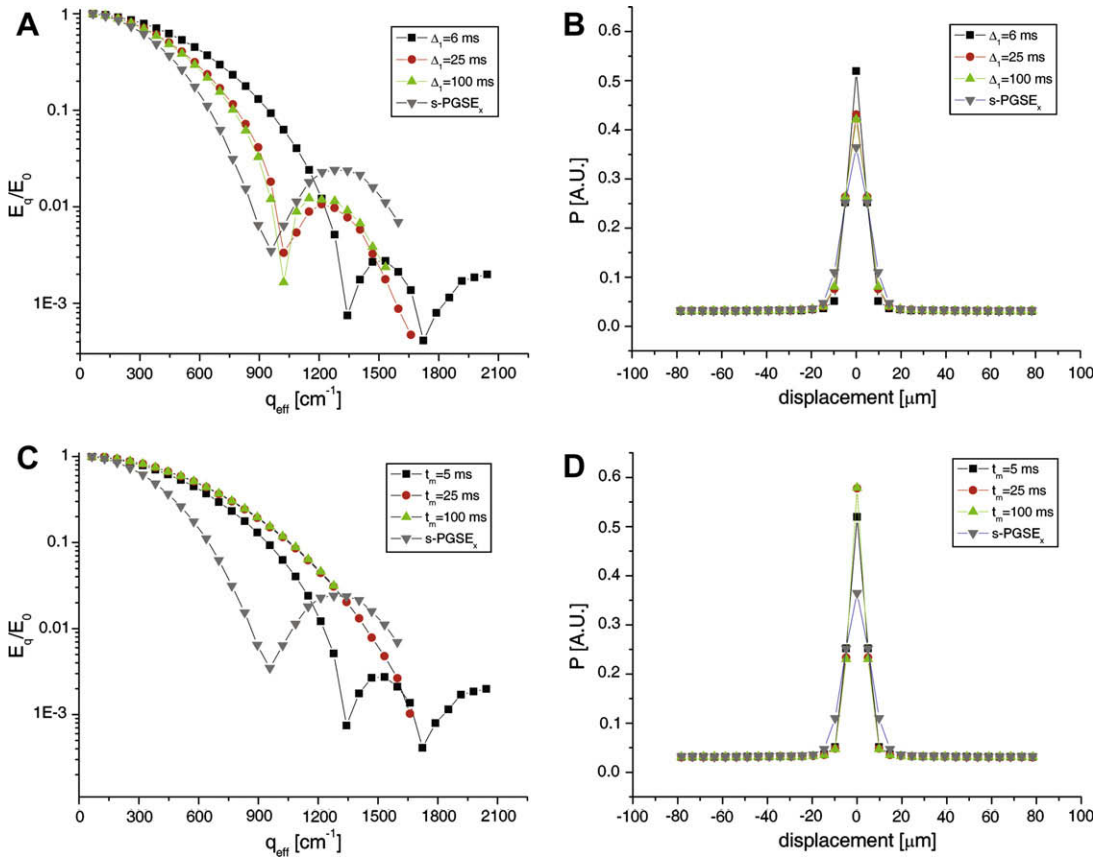

Fig. 8. Signal decay as a function of q_{eff} (A and C) and the FT of the signal decay (B and D) of d-PGSE$_{xx}$ experiments performed on a sample containing a mixture of 3:1 15:20 μm microcapillaries. (A and B) The first diffusion period was varied while Δ_2 was set to 100 ms, and the mixing time was set to 5 ms. (C and D) The diffusion periods were set to Δ_1 = 6 ms, Δ_2 = 100 ms and the mixing time (t_m) was varied as indicated. The results from the s-PGSE$_x$ experiment are also shown. Note that the s-PGSE results are plotted versus q.

corresponds fairly well with the ratio of 29/20. In both samples, we could not discriminate between the two sizes from the displacement profile obtained from the FT of the signal decay (Fig. 7B).

In the case of the second mixture, i.e., 3:1 15:20 μm (Fig. 8), the s-PGSE$_x$ showed a bias towards the more abundant size, but the diffraction was not sharp and clear, and one cannot tell that there are microcapillaries of two sizes in the sample. The diffraction dip occurs at q = 958 cm^{-1}, corresponding to a size of 12.7 μm. When we set Δ_2 to 100 ms while the t_m was 5 ms and varied Δ_1 (Fig. 8A and B), we found that when Δ_1 = 6 ms, two diffraction dips were observed at q_{eff} = 1342 and 1723 cm^{-1}, corresponding to sizes of 9.1 and 7.1 μm. Interestingly, here again the ratio corresponds to ~20/15. When Δ_1 was further prolonged, the d-PGSE$_{xx}$ signal lost the second diffraction, and the first diffraction shifted to lower q values to q_{eff} = 1021 cm^{-1}, corresponding to a size of 12.0 μm. Since we suspected that the effect of prolonging the mixing time in collinear d-PGSE$_{xx}$ experiments corresponds to the effect of increasing δ, we repeated the experiments with different t_m values, as shown in Fig. 8C and D. Prolonging the mixing time reveals a shift to higher q values which seem to reach an asymptotic value. These results indicate that indeed, under certain experimental conditions, the d-PGSE experiment can characterize samples with different sizes better than s-PGSE. However, it should be noted that the diffraction patterns are highly sensitive to the diffusion and mixing time, and that the sizes that were extracted did not reveal the actual sizes in the sample (but smaller sizes) probably due to the effect of the finite length of the pulsed gradients and the non-zero mixing time.

4. Conclusions

In this paper, we have evaluated the effect of different parameters on the signal decay and the structural information extracted thereof when the d-PGSE experiment is used to characterize water filled microcapillaries. We have shown for the first time that negative diffractions are, in fact, obtained in the d-PGSE$_{xx}$ experiments. We have shown the differential effect of the mixing time in orthogonal and collinear experiments, as well as the effect of changing the diffusion periods, and their order. Indeed, the signal decay and the structural information that may be obtained by the d-PGSE are dependant on these parameters. When certain experimental conditions are met, the structural information obtained from the d-PGSE experiment may surpass that of the s-PGSE, especially in the context of mixtures. We have found that under these circumstances, the d-PGSE can better characterize samples with a variance in size. Thus, the d-PGSE sequence may be of importance in studying non-isotropic diffusion in other systems such as biological tissues, as well as heterogeneous materials.

References

[1] E.O. Stejskal, J.E. Tanner, Spin diffusion measurements – spin echoes in presence of a time-dependent field gradient, J. Chem. Phys. 42 (1965) 288–292.
[2] P. Stilbs, Fourier transform pulsed-gradient spin-echo studies of molecular diffusion, Prog. Nucl. Magn. Reson. Spectrosc. 19 (1987) 1–45.
[3] Y. Cohen, L. Avram, L. Frish, Diffusion NMR spectroscopy in supramolecular and combinatorial chemistry: an old parameter – new insights, Angew. Chem., Int. Ed. 44 (2005) 520–554.

[4] P.S. Pregosin, P.G.A. Kumar, I. Fernandez, Pulsed gradient spin-echo (PGSE) diffusion and H-1,F-19 heteronuclear over Hauser spectroscopy (HOESY) NMR methods in inorganic and organometallic chemistry: something old and something new, Chem. Rev. 105 (2005) 2977–2998.
[5] A. Dehner, H. Kessler, Diffusion NMR spectroscopy: folding and aggregation of domains in p53, ChemBioChem 6 (2005) 1550–1565.
[6] P.T. Callaghan, NMR imaging, NMR diffraction and applications of pulsed gradient spin echoes in porous media, Magn. Reson. Imaging 14 (1996) 701–709.
[7] A. Coy, P.T. Callaghan, Pulsed gradient spin-echo NMR diffusive diffraction experiments on water surrounding close-packed polymer spheres, J. Colloid Interface Sci. 168 (1994) 373–379.
[8] D. LeBihan, Molecular diffusion, tissue microdynamics and microstructure, NMR Biomed. 8 (1995) 375–386.
[9] P.T. Callaghan, D. Macgowan, K.J. Packer, F.O. Zelaya, High-resolution *Q*-space imaging in porous structures, J. Magn. Reson. 90 (1990) 177–182.
[10] P.T. Callaghan, A. Coy, D. Macgowan, K.J. Packer, F.O. Zelaya, Diffraction-like effects in NMR diffusion studies of fluids in porous solids, Nature 351 (1991) 467–469.
[11] P.T. Callaghan, Pulsed-gradient spin-echo NMR for planar, cylindrical, and spherical pores under conditions of wall relaxation, J. Magn. Reson. Ser. A 113 (1995) 53–59.
[12] W.S. Price, Pulsed-field gradient nuclear magnetic resonance as a tool for studying translational diffusion. 1. Basic theory, Concepts Magn. Reson. 9 (1997) 299–336.
[13] P.T. Callaghan, S.L. Codd, J.D. Seymour, Spatial coherence phenomena arising from translational spin motion in gradient spin echo experiments, Concepts Magn. Reson. 11 (1999) 181–202.
[14] S.L. Codd, P.T. Callaghan, Spin echo analysis of restricted diffusion under generalized gradient waveforms: planar, cylindrical, and spherical pores with wall relaxivity, J. Magn. Reson. 137 (1999) 358–372.
[15] D.G. Cory, A.N. Garroway, Measurement of translational displacement probabilities by NMR – an indicator of compartmentation, Magn. Reson. Med. 14 (1990) 435–444.
[16] A.V. Barzykin, Theory of spin echo in restricted geometries under a step-wise gradient pulse sequence, J. Magn. Reson. 139 (1999) 342–353.
[17] B.N. Ryland, P.T. Callaghan, Spin echo analysis of restricted diffusion under generalized gradient waveforms for spherical pores with relaxivity and interconnections, Isr. J. Chem. 43 (2003) 1–7.
[18] L. Avram, E. Özarslan, Y. Assaf, A. Bar-Shir, Y. Cohen, P.J. Basser, Three-dimensional water diffusion in impermeable cylindrical tubes: theory versus experiments, NMR Biomed. 21 (2008) 888–898.
[19] A. Caprihan, L.Z. Wang, E. Fukushima, A multiple-narrow-pulse approximation for restricted diffusion in a time-varying field gradient, J. Magn. Reson. Ser. A 118 (1996) 94–102.
[20] D. Topgaard, O. Soderman, Experimental determination of pore shape and size using *q*-space NMR microscopy in the long diffusion-time limit, Magn. Reson. Imaging 21 (2003) 69–76.
[21] L. Avram, Y. Assaf, Y. Cohen, The effect of rotational angle and experimental parameters on the diffraction patterns and micro-structural information obtained from *q*-space diffusion NMR: implication for diffusion in white matter fibers, J. Magn. Reson. 169 (2004) 30–38.
[22] P.W. Kuchel, A. Coy, P. Stilbs, NMR "diffusion–diffraction" of water revealing alignment of erythrocytes in a magnetic field and their dimensions and membrane transport characteristics, Magn. Reson. Med. 37 (1997) 637–643.
[23] A.M. Torres, R.J. Michniewicz, B.E. Chapman, G.A.R. Young, P.W. Kuchel, Characterisation of erythrocyte shapes and sizes by NMR diffusion–diffraction of water: correlations with electron micrographs, Magn. Reson. Imaging 16 (1998) 423–434.
[24] M.D. King, J. Houseman, S.A. Roussel, N. Vanbruggen, S.R. Williams, D.G. Gadian, *Q*-space imaging of the brain, Magn. Reson. Med. 32 (1994) 707–713.
[25] M.D. King, J. Houseman, D.G. Gadian, A. Connelly, Localized *q*-space imaging of the mouse brain, Magn. Reson. Med. 38 (1997) 930–937.
[26] Y. Assaf, A. Mayk, Y. Cohen, Displacement imaging of spinal cord using *q*-space diffusion-weighted MRI, Magn. Reson. Med. 44 (2000) 713–722.
[27] Y. Assaf, D. Ben-Bashat, J. Chapman, S. Peled, I.E. Biton, M. Kafri, Y. Segev, T. Hendler, A.D. Korczyn, M. Graif, Y. Cohen, High *b*-value *q*-space analyzed diffusion-weighted MRI: application to multiple sclerosis, Magn. Reson. Med. 47 (2002) 115–126.
[28] R. Nossin-Manor, R. Duvdevani, Y. Cohen, Effect of experimental parameters on high *b*-value *q*-space MR images of excised rat spinal cord, Magn. Reson. Med. 54 (2005) 96–104.
[29] I.E. Biton, I.D. Duncan, Y. Cohen, q-space diffusion of myelin-deficient spinal cords, Magn. Reson. Med. 58 (2007) 993–1000.
[30] J.A. Farrell, S.A. Smith, E.M. Gordon-Lipkin, D.S. Reich, P.A. Calabresi, P.C. van Zijl, High *b*-value *q*-space diffusion-weighted MRI of the human cervical spinal cord in vivo: feasibility and application to multiple sclerosis, Magn. Reson. Med. 59 (2008) 1079–1089.
[31] A. Bar-Shir, Y. Cohen, High *b*-value *q*-space diffusion MRS of nerves: structural information and comparison with histological evidence, NMR Biomed. 21 (2008) 165–174.
[32] H.H. Ong, A.C. Wright, S.L. Wehrli, A. Souza, E.D. Schwartz, S.N. Hwang, F.W. Wehrli, Indirect measurement of regional axon diameter in excised mouse spinal cord with *q*-space imaging: simulation and experimental studies, Neuroimage 40 (2008) 1619–1632.
[33] S. Peled, D.G. Cory, S.A. Raymond, D.A. Kirschner, F.A. Jolesz, Water diffusion, T-2, and compartmentation in frog sciatic nerve, Magn. Reson. Med. 42 (1999) 911–918.
[34] D.G. Cory, A.N. Garroway, J.B. Miller, Applications of spin transport as a probe of local geometry, Polym. Preprints 31 (1990) 149.
[35] P.P. Mitra, Multiple wave-vector extensions of the NMR pulsed-field-gradient spin-echo diffusion measurement, Phys. Rev. B 51 (1995) 15074–15078.
[36] P.T. Callaghan, A.A. Khrapitchev, Time-dependent velocities in porous media dispersive flow, Magn. Reson. Imaging 19 (2001) 301–305.
[37] P.T. Callaghan, S. Godefroy, B.N. Ryland, Use of the second dimension in PGSE NMR studies of porous media, Magn. Reson. Imaging 21 (2003) 243–248.
[38] B. Blumich, P.T. Callaghan, R.A. Damion, S. Han, A.A. Khrapitchev, K.J. Packer, S. Stapf, Two-dimensional NMR of velocity exchange: VEXSY and SERPENT, J. Magn. Reson. 152 (2001) 162–167.
[39] A. Jerschow, N. Muller, Suppression of convection artifacts in stimulated-echo diffusion experiments. Double-stimulated-echo experiments, J. Magn. Reson. 125 (1997) 372–375.
[40] P.T. Callaghan, M.E. Komlosh, Locally anisotropic motion in a macroscopically isotropic system: displacement correlations measured using double pulsed gradient spin-echo NMR, Magn. Reson. Chem. 40 (2002) S15–S19.
[41] M.E. Komlosh, F. Horkay, R.Z. Freldlin, U. Nevo, Y. Assaf, P.J. Basser, Detection of microscopic anisotropy in gray matter and in a novel tissue phantom using double pulsed gradient spin echo MR, J. Magn. Reson. 189 (2007) 38–45.
[42] M.E. Komlosh, M.J. Lizak, F. Horkay, R.Z. Freidlin, P.J. Basser, Observation of microscopic diffusion anisotropy in the spinal cord using double-pulsed gradient spin echo MRI, Magn. Reson. Med. 59 (2008) 803–809.
[43] E. Özarslan, P.J. Basser, MR diffusion–diffraction phenomenon in multi-pulse-field-gradient experiments, J. Magn. Reson. 188 (2007) 285–294.
[44] E. Özarslan, P.J. Basser, Microscopic anisotropy revealed by NMR double pulsed field gradient experiments with arbitrary timing parameters, J. Chem. Phys. 128 (2008) 154511.